



Cerebrovascular Reactivity Has Negligible Contribution to Hemodynamic Lag After Stroke: Implications for Functional Magnetic Resonance Imaging Studies

Andra Braban, MSc; Robert Leech¹, PhD; Kevin Murphy, PhD; Fatemeh Geranmayeh¹, PhD

BACKGROUND: Functional magnetic resonance imaging (fMRI) is ubiquitously used to study poststroke recovery. However, the fMRI-derived hemodynamic responses are vulnerable to vascular insult which can result in reduced magnitude and temporal delays (lag) in the hemodynamic response function (HRF). The cause of HRF lag remains controversial, and a better understanding of it is required to ensure accurate interpretation of poststroke fMRI studies. In this longitudinal study, we investigate the relationship between hemodynamic lag and cerebrovascular reactivity (CVR) following stroke.

METHODS: Voxel-wise lag maps were calculated relative to a mean gray matter reference signal for 27 healthy controls and 59 patients with stroke across 2 time points (≈ 2 weeks and ≈ 4 months poststroke) and 2 conditions: resting-state and breath-holding. The breath-holding condition was additionally used to calculate CVR in response to hypercapnia. HRF lag was computed for both conditions across tissue compartments: lesion, perilesional tissue, unaffected tissue of the lesioned hemisphere, and their homolog regions in the unaffected hemisphere. CVR and lag maps were correlated. Group, condition, and time effects were assessed using ANOVA analyses.

RESULTS: Compared with the average gray matter signal, a relative hemodynamic lead was observed in the primary sensorimotor cortices in resting-state and bilateral inferior parietal cortices in the breath-holding condition. Whole-brain hemodynamic lag was significantly correlated across conditions irrespective of group, with regional differences across conditions suggestive of a neural network pattern. Patients showed relative lag in the lesioned hemisphere which significantly reduced over time. Breath-hold derived lag and CVR had no significant voxel-wise correlation in controls, or patients within the lesioned hemisphere or the homologous regions of the lesion and perilesional tissue in the right hemisphere (mean $r < 0.1$).

CONCLUSIONS: The contribution of altered CVR to HRF lag was negligible. We suggest that HRF lag is largely independent of CVR, and could partly reflect intrinsic neural network dynamics among other factors.

GRAPHIC ABSTRACT: A [graphic abstract](#) is available for this article.

Key Words: gray matter ■ hemodynamic ■ magnetic resonance imaging ■ stroke

Resting-state (RS) functional magnetic resonance imaging (fMRI) has become instrumental in enhancing our understanding of mechanisms of poststroke functional recovery. The fMRI-derived blood

oxygen level-dependent (BOLD) signal is modeled through the hemodynamic response function (HRF) and is contingent on intact neurovascular coupling.¹ Two key properties of the HRF are its temporal delay

Correspondence to: Fatemeh Geranmayeh, PhD, Clinical Language and Cognition Group, Imperial College London, W120NN, United Kingdom. Email fatemeh.geranmayeh00@imperial.ac.uk

Supplemental Material is available at <https://www.ahajournals.org/doi/suppl/10.1161/STROKEAHA.122.041880>.

For Sources of Funding and Disclosures, see page 1076.

© 2023 The Authors. *Stroke* is published on behalf of the American Heart Association, Inc., by Wolters Kluwer Health, Inc. This is an open access article under the terms of the [Creative Commons Attribution](#) License, which permits use, distribution, and reproduction in any medium, provided that the original work is properly cited.

Stroke is available at www.ahajournals.org/journal/str

Nonstandard Abbreviations and Acronyms

BH	breath-hold
BOLD	blood oxygen level–dependent
CVR	cerebrovascular reactivity
fMRI	functional magnetic resonance imaging
HRF	hemodynamic response function
HV	healthy volunteers
ROI	region of interest
RS	resting-state

(lag) and magnitude. The former is calculated by cross-correlation with a reference signal (eg, average gray matter signal) to derive a relative lead or lag, whereas the latter is used to measure cerebrovascular reactivity (CVR) in response to a vasoactive stimulus.

BOLD signal temporal delays, including a relative lead or lag, have been observed in health² and after stroke.^{3–7} Specifically, RS temporal lags following stroke (1) have been identified in areas of abnormal perfusion,^{3–5,8} and positively correlate with stroke lesion size,⁷ (2) have been shown to extend beyond the lesion boundary in brain regions displaying altered hemodynamic flow,^{3,6,7} (3) may confound observed changes in functional connectivity,⁶ and (4) may explain variability in behavioral outcomes after stroke.⁷ Given the ubiquitous use of fMRI in post-stroke recovery literature and the vulnerability of BOLD signal to vascular insult, a better understanding of the mechanisms underpinning hemodynamic lag is needed for accurate interpretation of such studies in stroke.

Several factors have been proposed to contribute to hemodynamic lag observed in stroke which are not necessarily mutually exclusive. First, lag may be seen in indirectly affected regions that share a vascular supply with the lesioned area.^{3,5,6} Although some studies in patients with hyperacute⁸ or subacute⁶ stroke have demonstrated a correlation between perfusion metrics and hemodynamic lag, studies in large healthy cohorts, where observed lag is typically of lower magnitude, have not confirmed this.² Furthermore, a study in healthy controls only showed perfusion-related correlations with regions of hemodynamic delay rather than lead.⁹ Equally, although studies have shown recovery of lag with reperfusion after recanalization in the hyperacute/acute phase of stroke,¹⁰ others investigating lag recovery in the subacute phase, have not.⁶

A second hypothesis suggests that hemodynamic lag is partly determined by the intrinsic temporal dynamics at the level of the functional neural networks² and may be hard-wired by the underlying structural connectivity between brain regions.¹¹ This change in lag may be in the order of 1 second, based on studies on healthy controls²; however, extrapolating this evidence to patients

with stroke can be precarious. In practice, disentangling the relative contributions of neural versus vascular processes to hemodynamic lag is challenging using fMRI alone, particularly in aging and diseased states.

A third plausible explanation for hemodynamic lag observed in nonlesioned brain, and one that will be the subject of this study is neurovascular decoupling. It is well established that stroke disrupts neurovascular coupling,^{12,13} primarily due to ischemia-sensitive glial dysfunction.^{6,14,15} The vascular response to a given change in neural activity can be affected by alterations in CVR. CVR represents the vasodilatory response of cerebral microvasculature to increased metabolic demands, quantified in response to a vasodilatory trigger such as hypercapnia.^{16–20} Specifically, CVR can be quantified as %BOLD signal change per unit change in end-tidal CO₂ in response to hyperventilation²¹ or breath-holding.²² The breath-holding paradigm produces robust and repeatable measures of CVR even in suboptimal performance of the breath-holding task (eg, in patients).¹⁶ We have previously shown that CVR is reduced within the lesioned and perilesional tissue immediately after stroke, with no recovery into the chronic phase.²²

In this novel longitudinal study, we directly investigate the extent to which the fMRI BOLD signal temporal lags are related to potential reductions in CVR after stroke. We compare hemodynamic lags in a cohort of patients with left hemisphere stroke, and aged-matched healthy controls, at subacute and chronic stages after stroke and during 2 conditions (RS and BH). We show that despite group-level regional differences in lag across conditions, there is a significant whole-brain spatial correlation between the RS and breath-holding derived lag. Furthermore, we show that the spatial correlation between lag and CVR maps is not significant in controls nor is it significant in the lesioned hemisphere or homologous lesion and perilesional tissue contralesionally. We suggest that alterations in CVR poststroke have negligible effects on alterations in HRF lag and argue that lag differences may be partly driven by differential neural network dynamics. Finally, we show that lag measurements are highly consistent irrespective of the reference signal chosen for lag calculation. The results of this study will improve our ability to interpret fMRI data from patients after stroke.

METHODS

The data are available from the corresponding author upon reasonable request.

Participant Recruitment

RS and BH fMRI data were acquired from 59 patients following a left hemisphere infarct and 27 age and sex-matched healthy volunteers (HV). Participants performed additional language task fMRI as part of a larger study published previously.^{23–25} Inclusion/exclusion criteria are described in

Supplemental Methods. Patients underwent scanning in the subacute (V1-visit 1: \approx 2 weeks), and chronic (V2-visit 2: \approx 4 months) phase post ictus. The National Research Ethics Service Committee approved the study. All participants provided written informed consent.

FMRI Paradigms

During the BH task, participants completed 6 BH cycles, consisting of 14 s of normal breathing, 16 s of paced breathing, and 15 s of end-expiration BH, followed by return to normal breathing.²² The RS fMRI was performed with eyes closed. All included participants confirmed they were alert postscan.

Neuroimaging Data Acquisition and Preprocessing

FMRI and T1-weighted structural MRI data were acquired using Siemens Magnetom Trio3 scanner (see [Supplemental Methods](#) for details). RS and BH images were preprocessed (nonbrain voxel removal, B0 unwarping, field map correction, high pass filter 0.01Hz, slice time correction, motion correction²⁶) and registered to standard space using FMRI Expert Analysis Tool 6.0.1, from FMRIB's Software Library. Six motion parameters and a cerebrospinal fluid time course were regressed from the preprocessed data. Outlier time points with excessive motion were identified as >1 mm movement in any direction²⁷ by framewise displacement and excluded. See [Supplemental Methods](#).

Hemodynamic Lag Calculation

Hemodynamic lags were calculated separately for RS and BH fMRI. Six scans (1 RS and 5 BH) from patients were excluded due to excessive motion ($>50\%$ of total acquired volume). Cohort numbers included in Figure 1A represent those remaining after these exclusions. For each individual, a binary segmented gray matter mask was created from the T1 image using FMRIB's Automated Segmentation Tool (3 classes, 4 iterations for bias field removal, 20 mm FWHM smoothing) and used to derive a reference time series from the preprocessed echoplanar images after lesion exclusion and transformation to echoplanar imaging space (Figure 1B, red).

For the hemodynamic lag calculation, the Lag-suite program⁶ was adapted and used in MATLAB R2021a. Motion outliers previously saved as separate regressors were applied to preprocessed echoplanar images to exclude frames with excessive motion. Lag was calculated by time-shifting each voxel's time series in 2-second increments by +8 s (forward shift) and -8 s (backward shift), representing ± 4 TRs, similar to previous studies.^{6,7,28} At each of the 9 shift positions, the signal was correlated with the reference signal. To prevent spurious correlations, voxels that did not display a minimum positive correlation with the gray matter signal ($r < 0.1$) were excluded, in keeping with previous studies.⁶ The excluded voxels were unsurprisingly predominantly located within the white matter (Figure S1). For each accepted voxel, the maximum cross-correlation value of the time-shifted signal, and the cross-correlation values at the neighboring shift positions were fitted into a parabolic function to compute the temporal shift corresponding to the maximum correlation (Figure 1C). The best-fit temporal shift, producing the maximum correlation, is the temporal hemodynamic change

(lead or lag) for that voxel. Given that lag and lead are relative time latencies measured against a reference signal, rather than an absolute value, they are expressed in units of time (seconds), in keeping with previous studies.^{2,6-10}

CVR Calculation

End-tidal CO₂ traces and global signal from all participants performing the BH task were inspected to ensure adequate breath-holding. In total 9 data points from 7 patients (3 at V1 and 6 at V2) were excluded from the CVR analysis due to suboptimal breath-hold. For the remaining 21 and 41 patients at V1 and V2 time point, respectively, CVR was calculated as %BOLD rise per unit of CO₂.²² A linear interpolation was made between the end-tidal CO₂ (sampling rate, 200 Hz) before and after each BH and convolved with a standard double gamma variate HRF. A time-shifted CO₂ trace, optimized for each voxel, was used as regressor in a General Linear Model using AFNI's 3dDeconvolve function. Voxel-wise optimization was performed to exclude delays between the BOLD data and CO₂ trace, caused by physiological processes or experimental setup. The CO₂ trace was systematically time-shifted between -15 s and +15 s in 0.1 s steps to find the best-fit delay for a given voxel, and this time-shifted trace was used as regressor in the General Linear Model. The BH response (units of %BOLD signal change per mmHg change in end-tidal CO₂) was calculated from the beta-weight for the given voxel and regressor (Figure 1C VoxOpt in Geranmayeh et al²²).

Group-Level Analyses

Group-level analyses of lag maps were conducted in FMRIB's Software Library by fitting a 2-way mixed-effect ANOVA (ordinary least squares method), to assess for a group, time point, and interaction effect (see [Supplemental Methods](#)). False discovery rate ($q=0.1$) was applied for multiple comparisons correction. An equivalent design was used to assess condition effect.

Correlation of Lag and CVR

A voxel-wise Spearman-rank correlation was used to assess the relationship between lag and CVR at subject-level in 3 tissue compartments: (1) lesion, where we have previously shown to have persistently reduced vascular reactivity after stroke²²; (2) perilesional tissue in close proximity to the infarcted area known to display abnormal BOLD signal,²⁹ hypoperfusion,³⁰ and reduced vascular reactivity.²² Perilesional tissue was arbitrarily defined within 1 cm of the lesion boundary and (3) healthy tissue remote from the former two. Homolog regions of interest (ROIs) were defined within the nonlesioned hemisphere (Figure 1D; ROI mask). Voxels displaying abnormal CVR response ($r < 0.1$) were excluded. Significance of correlation coefficients against 0 was assessed using a Wilcoxon signed-rank test ($\alpha=0.0083$ after Bonferroni correction for 6 ROIs). To further investigate the relationship between CVR and lag, a linear mixed-effect model with fixed effects for lag was applied (only r values are reported due to inherent high between-voxel signal autocorrelation).

Consistency of Hemodynamic Lag Across Conditions

RS and BH lag maps were spatially correlated using Pearson's correlation, restricted to each participant's functional space. A

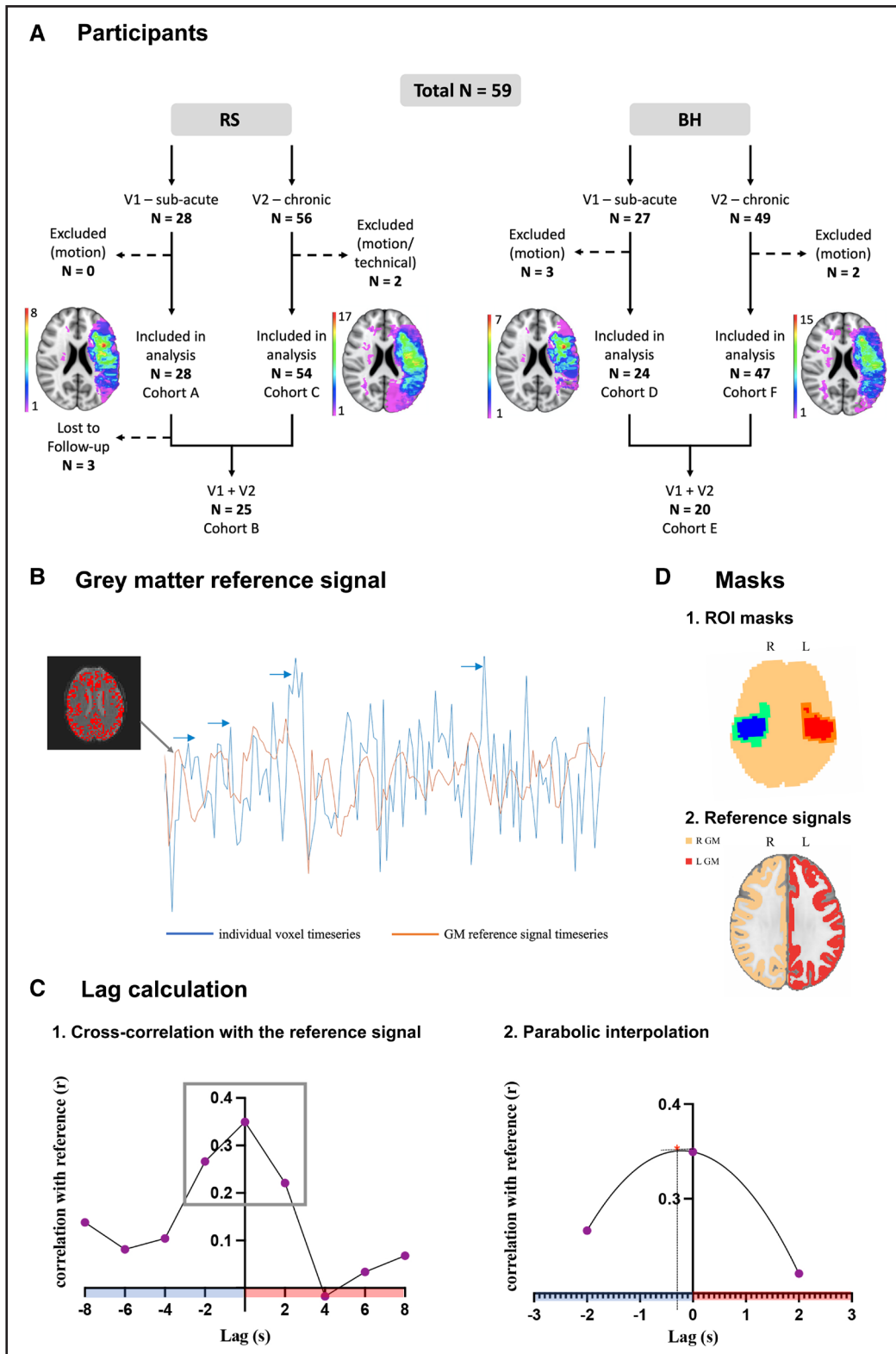


Figure 1. Methods.

A, Flow chart displaying number of patients included in each subcohort used for different functional magnetic resonance imaging (fMRI) lag analyses in the manuscript. All patients with breath-hold (BH) data also had resting-state (RS) data, except for 2 exclusions due to technical issues and motion. Lesion distributions for each subcohort are displayed. Color map indicates number of patients with lesion at each voxel. **B**, Lag was measured by shifting the time series of one voxel (blue), against that of the gray matter (GM) reference signal (orange). **C**, Correlation with reference at each shift position (**left**) and optimal lag calculation using parabolic interpolation (**right**). Positive and negative values indicate lag or lead respectively. **D**, Region of interest (ROI) masks for 1 patient (1). Masks used to calculate alternative reference signals (2). L indicates left; and R, right.

transformation matrix was calculated by transforming BH functional images to RS space using a rigid 3 degrees of freedom registration (FMRIB's Linear Image Registration Tool), and the resulting matrix was applied to the BH lag maps. Correlations were carried out in both groups at whole-brain level, and within ROIs including lesion, perilesional tissue, and remaining healthy tissue remote from the former 2 in patients. Group-level statistical analysis was conducted using Prism9.3.1 (GraphPad) and IBM SPSS Statistics24.

RESULTS

Participants

Imaging data were acquired from 59 patients (36 males, mean age \pm SD, 61.5 \pm 12.96 years) following a left hemisphere infarct, and 27 age and sex-matched HV (10 males, mean age \pm SD, 57.4 \pm 11.71 years). Due to stroke severity, only 47% of the patients were fit to undergo research fMRI in subacute phase (V1); therefore, data

were analyzed in subgroups which included different numbers of participants for each time point (Figure 1A; [Supplemental Methods](#)). Details of individual patients and subgroups are provided in [Tables S1](#) and [S2](#), respectively.

Group Differences in Hemodynamic Lag

The voxel-wise group mean lag maps were calculated for both RS and BH fMRI for each group and time point separately (Figure 2; [Figure S2](#)). Similar spatial distribution of lag was observed between groups. RS data showed a relative lead (blue) in bilateral sensorimotor cortices in precentral and postcentral gyri, middle and superior temporal gyri, precuneus, posterior cingulate cortex, dorsal and rostral anterior cingulate, and lateral occipital cortices ([Table S3](#)). The spatial extent of this relative lead appeared less pronounced in patients in the lesioned hemisphere compared with the nonlesioned hemisphere, hinting of a relative lag in patients.

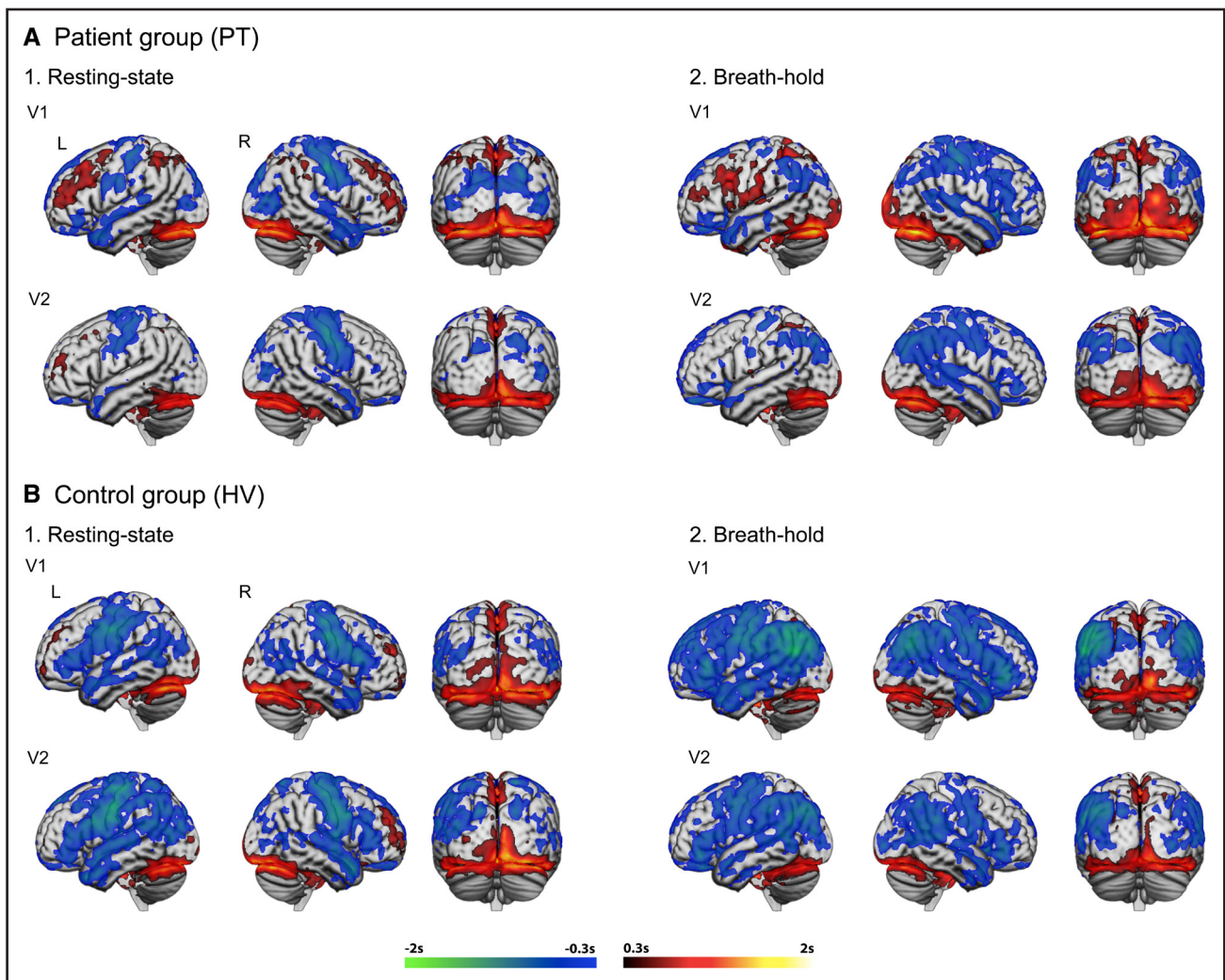


Figure 2. Mean gray matter hemodynamic lag (red-yellow) and lead (blue-green) greater than 0.3s in the 2 groups.

A, Patients (PT). **B**, Controls; resting-state (1); breath-hold (2); subacute phase (visit 1 [V1]); chronic phase (visit 2 [V2]). HV indicates healthy volunteers. L indicates left; and R, right.

In RS, areas of lag can be observed bilaterally in the midline occipito-parietal cortices, middle frontal gyri, and posterior precuneus cortices with a significant lag attributed to the transverse venous sinuses (Table S3). A similar pattern of lag/lead was observed during BH task (Figure 2, right), with more extensive relative lead in biparietal and bifrontal regions (see also results for regional differences across brain conditions).

Compared to controls, patients had higher variability in lag as shown by larger voxel-wise standard deviation of the hemodynamic lag, predominantly within the lesioned hemisphere (Figure S3). Two separate mixed-effect ANOVAs were performed for each condition (N=25 RS

cohort B, and N=20 BH cohort E in Figure 1A). A significant group effect on lag was observed in both conditions (Figure 3A.1–3). In RS, clusters of significantly higher lag in patients compared to controls were predominantly identified in the frontal and superior parietal lobes of the lesioned hemisphere, within the vascular territory of the stroke, but peripheral to areas of largest group-level lesion density (Figure 3A.3). Areas with significantly more lead in patients were observed in the bilateral occipital cortices (Figure 3A.1 coronal). Similar results were observed in the breath-holding condition, with significant lag in patients ipsilesionally in the frontal lobe, precentral and postcentral gyri, and temporal lobe (Figure 3A.2).

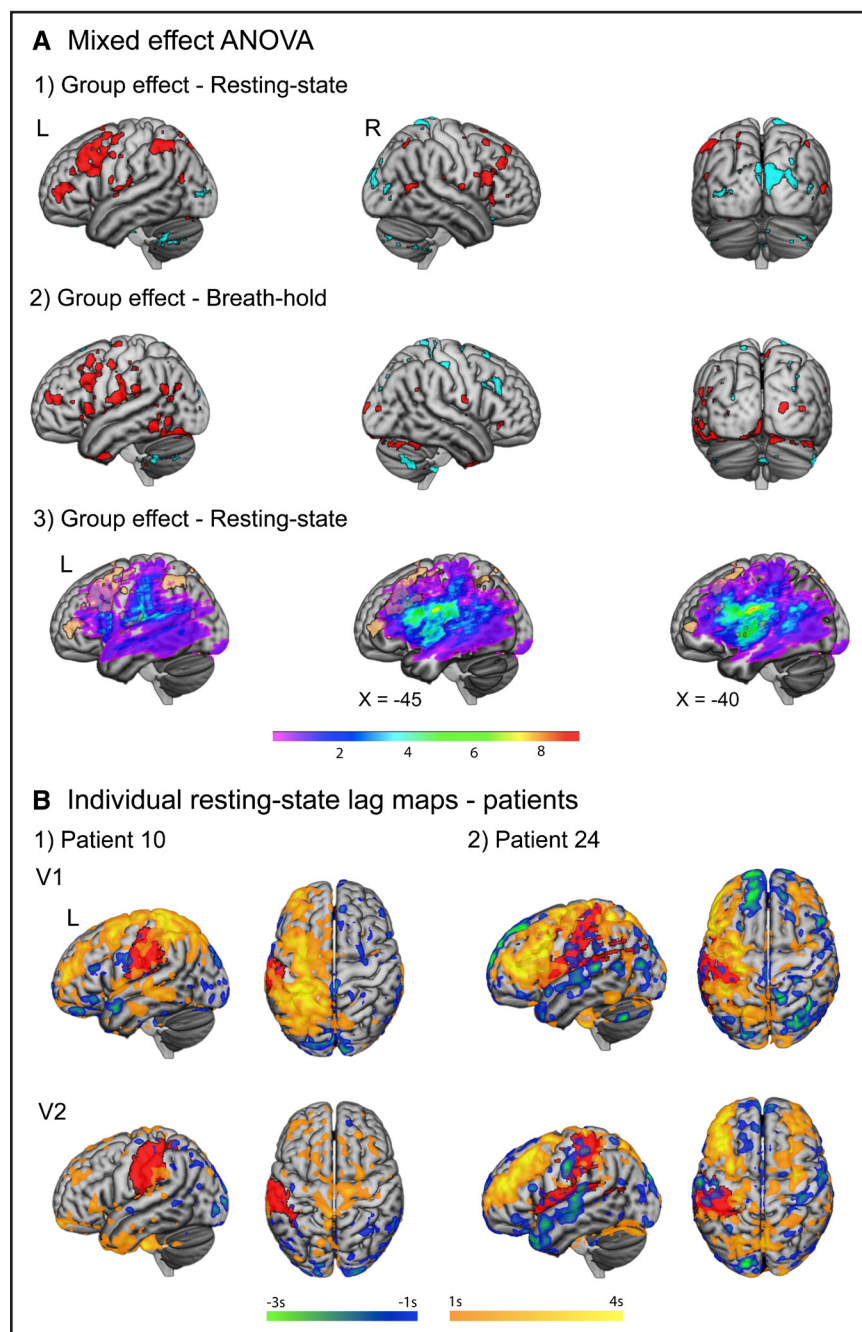


Figure 3. Group-level analyses and individual lag maps. **A**, Two-way mixed-effect ANOVA results assessing for group differences in gray matter lag during resting-state (RS; 1) and breath-hold (2), false discovery rate corrected. Red and blue clusters (A.1,2) indicate areas of significantly more lag (primarily ipsilesionally) and lead respectively, in patients compared to controls. Lesion overlap (A.3) demonstrates that clusters of significant lag in patients (light brown) are found outside regions of highest lesion density. Color map indicates group-level lesion density. **B**, RS lag maps for 2 example patients, subacutely (visit 1 [V1]) and chronically (visit 2 [V2]). Lag maps show lag (yellow) and lead (blue) >1 s. Lesions are displayed in red. L indicates left; and R, right.

Downloaded from <http://ahajournals.org> by on April 17, 2023

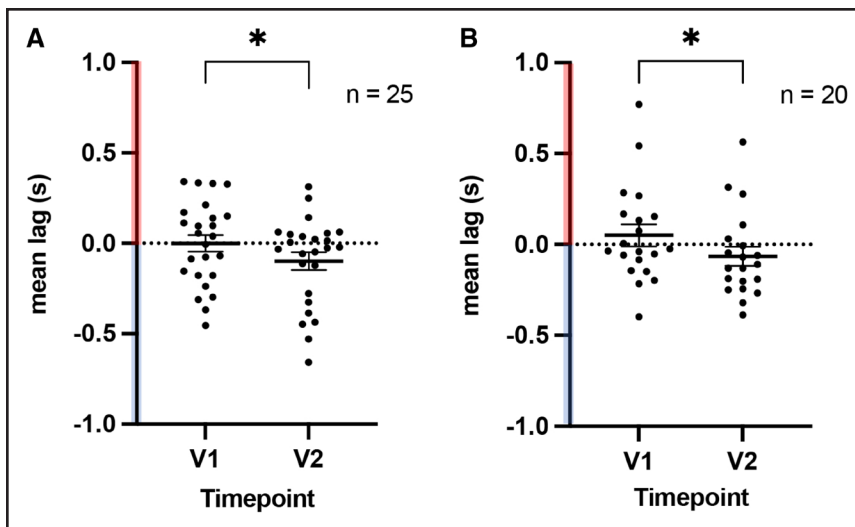


Figure 4. Mean hemodynamic lag in the lesioned hemisphere gray matter, in the sub-acute (V1) and chronic (V2) phase of stroke (cohorts B and E).

A, Resting-state. **B**, Breath-hold. A partial resolution of lag was observed in the chronic phase ($*P < 0.03$). Pink and blue on Y axis refer to lag and lead respectively; mean \pm SEM displayed.

Lag Within the Lesioned Hemisphere Is Partially Reversed Over Time After Stroke

The extent of the lag within the lesioned hemisphere and its recovery were variable in patients (Figure S3). Figure 3B shows 2 representative examples with different patterns of lag recovery over time. Interestingly, patient 10 had complete occlusion of the left middle cerebral artery but showed more reduction of lag in the lesioned hemisphere when compared with patient 24, who had relatively less lag reduction over time. Despite idiosyncratic patterns of change in lag in patients, group-level calculation of mean gray matter lag within the lesioned hemisphere in cohorts B (RS-V1: -0.0001 ± 0.23 s [mean \pm SD]; V2: -0.099 ± 0.24 s) and E (BH-V1: 0.05 ± 0.27 s; V2: -0.065 ± 0.23 s) showed a significant reduction of lag over time (1-tailed t test $P = 0.0284$ and $P = 0.0166$, respectively; Figure 4). This suggests that at group-level, across both conditions, lag in the stroke-affected hemisphere partially reduced over months after the stroke. This was driven by 14 out of 25 and 14 out of 20 patients in the RS and BH cohorts respectively that showed a reduction in the absolute lag value in the left hemisphere over time.

CVR Has Minimal Contribution to the Observed fMRI Lag

The main purpose of this study was to investigate the relationship between fMRI lag (calculated against the gray matter reference signal) and CVR (measured separately as %BOLD signal change per unit rise in end-tidal CO_2). Voxel-wise Spearman correlation between BH fMRI lag and CVR for each participant and different ROIs are shown in Figure 5 (also see Figure S4 for absolute CVR values). There was no significant correlation (mean r range = -0.06 to 0.02 , Wilcoxon signed-rank $P > 0.01$, $\alpha = 0.0083$ Bonferroni correction) between lag and CVR within the lesion and perilesional tissue and their homologous right hemisphere

regions, or healthy brain tissue remote from the lesion in the left hemisphere, at either time point (Figure 5A and 5B). Right hemisphere brain tissue remote from the lesion homolog showed minimal, nevertheless significant, correlation between lag and CVR at the 2 time points (V1 subject-level voxel-wise spatial correlation mean < 0.05 , Wilcoxon signed-rank $P < 0.01$; V2 mean < 0.05 , $P < 0.001$). No significant correlation was observed in controls (Wilcoxon signed-rank $P > 0.3$).

A linear mixed-effect model (Figure 5C and 5D) confirmed very small fixed-effect coefficients in the right remote healthy tissue (V1: 0.0139 ; V2: 0.0145), suggesting that very little variance in lag is explained by CVR.

fMRI Lag Is Spatially Correlated Across Brain Conditions, With Some Regional Differences

Within participants ($N = 20$ patients cohort E and 17 HV), lag maps derived from the 2 conditions were correlated across both groups and time points (Figure 6A). Mean subject-level voxel-wise spatial correlation were $r = 0.21$ (patients-V1) and 0.23 (patients-V2) $r = 0.16$ (HV-V1) and 0.19 (HV-V2), all $P < 0.0001$ 1-sample t test. Similar significant correlations were observed within individual ROIs chosen in relation to lesion in patients (Figure 6B; 1-sample t tests $P < 0.0007$). A 2-way repeated measure ANOVA was further performed to assess for an effect of group and time point on the spatial correlation between lag maps derived from the 2 conditions. Results showed no significant effect of group ($F[1,35] = 1.872$, $P = 0.18$), time point ($F[1,35] = 3.158$, $P = 0.0842$), or interaction ($F[1,35] = 0.3053$, $P = 0.5841$), suggesting consistency of the similarity of lag maps in the 2 conditions (Figure 6A). Similarly, ROI analysis in the patient group showed no significant effect of region ($F[1.552,29.5] = 2.973$, $P = 0.0782$), time point ($F(1,19) = 0.3044$, $P = 0.5876$), or interaction ($F[1.973,37.50] = 1.72$, $P = 0.1932$) on the spatial correlations (Figure 6B).

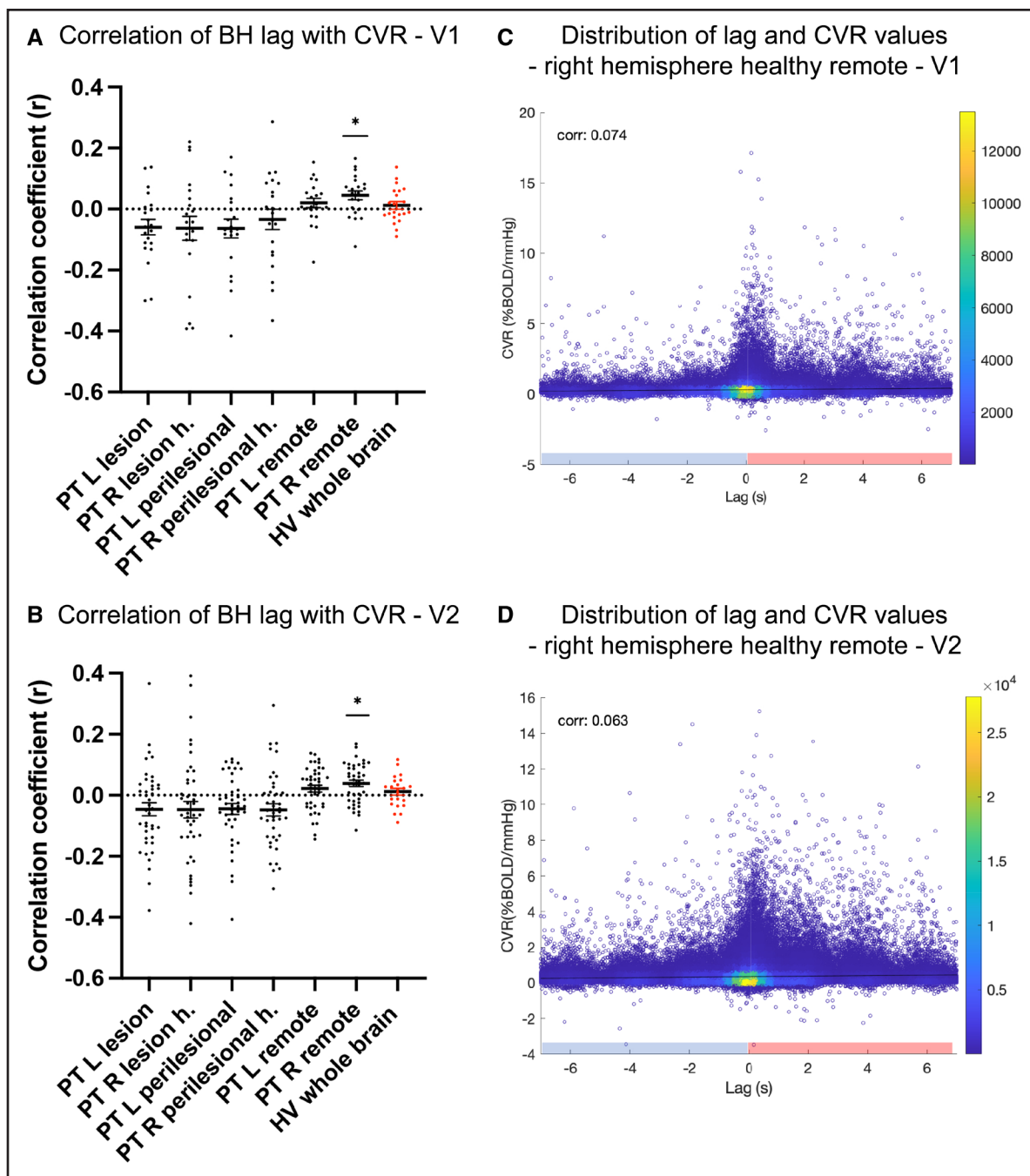


Figure 5. Cerebrovascular reactivity (CVR) contribution to the functional magnetic resonance imaging (fMRI) lag. Spearman-rank correlation between individual participant's lag and CVR maps, in patients (PT; black) and controls (red), at visit 1 (V1; **A**), and visit 2 (V2; **B**). Mean±SEM displayed. Distribution of voxel-level lag and CVR values within healthy remote brain tissue of the right hemisphere at V1 (**C**) and V2 (**D**) shown for all PT. Color map shows the relative density of data points. Pink and blue on x axis refer to lag and lead respectively. BH indicates breath-hold; CVR, cerebrovascular reactivity; HV, healthy volunteers; L, left; PT, patients; and R, right.

Given all above, the lag maps across the 2 conditions were generally spatially similar. Nevertheless, a 2-way mixed-effects ANOVA (Figure 6C) revealed regional differences in lag between brain conditions. Clusters where the breath-holding condition showed increased lead compared to RS were starkly similar to regions commonly coactivated as part of the multiple demand cortex³¹ and frontoparietal attentional networks,³² including the bilateral

anterior and dorsolateral prefrontal cortex, midcingulate and right anterior insula/frontal operculum cortices, and bilateral inferior parietal lobules (Figure 6C; Table S4).

DISCUSSION

This is the first study that has directly tested the relationship between CVR and fMRI hemodynamic lag

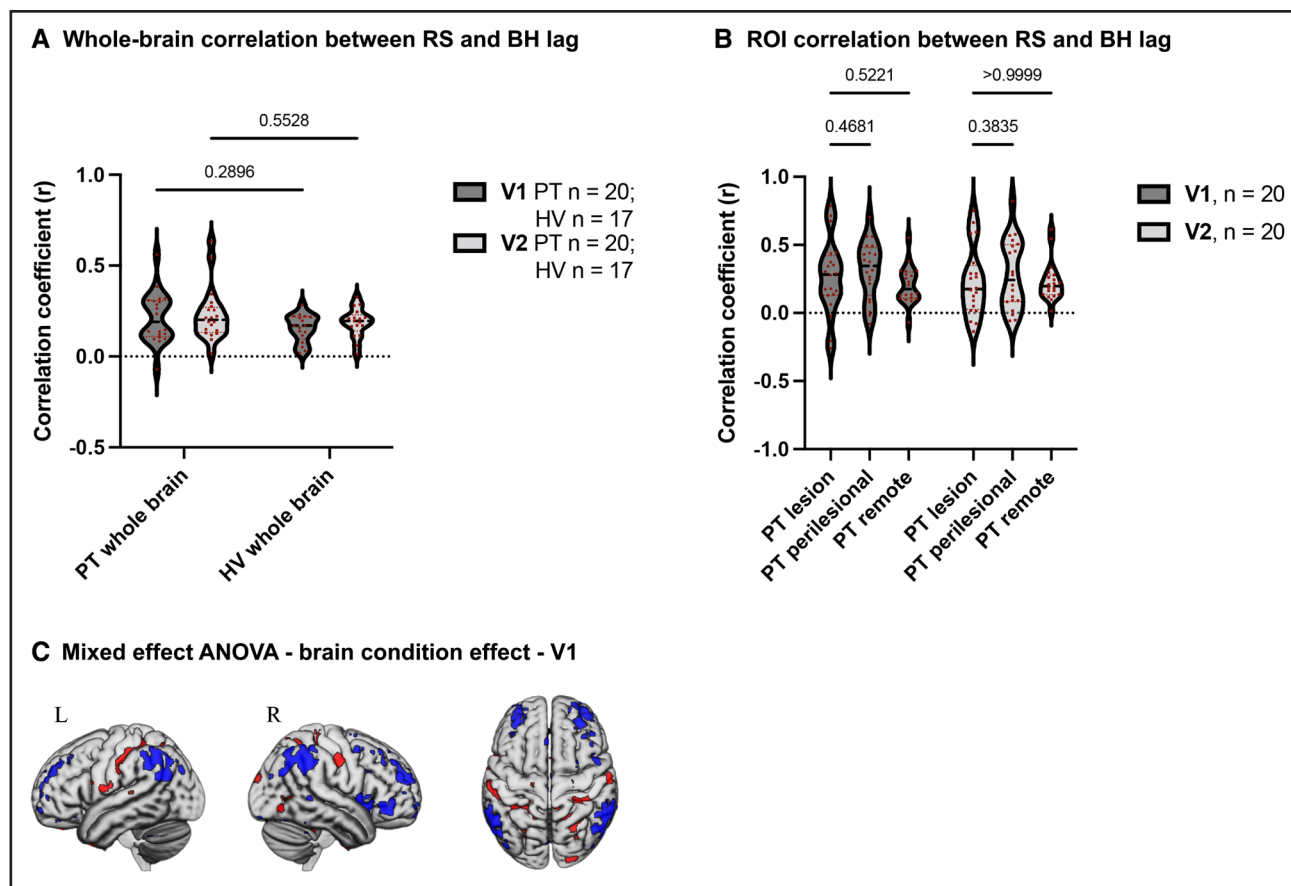


Figure 6. Differences in lag across brain conditions (resting-state [RS] and breath-hold [BH]).

There was a consistent similarity of lag maps derived from 2 brain states in patients and controls (A) and within regions of interest in the patient group (B). C, Two-way mixed-effect ANOVA assessing differences in lag across brain conditions (visit 1 [V1]), false discovery rate corrected. Blue and red clusters show a significantly greater lead and lag respectively, in breath-hold compared with resting-state. V2 indicates visit 2. HV indicates healthy volunteers; L, left; PT, patients; R, right; and ROI, region of interest.

longitudinally after stroke. The results support the view that CVR has negligible contribution to the hemodynamic lag. We demonstrated no significant relationship between the 2 measures within the lesion and perilesional tissue, their homologous regions within the nonlesioned hemisphere, in the remote healthy tissue of the lesioned hemisphere, or indeed in controls at whole-brain level in whom CVR would be expected to be normal. Although a small but significant positive correlation was seen between CVR and lag within the remote healthy brain regions of the right hemisphere, CVR explained very little in the variability of the observed hemodynamic lag in our data, suggesting it has an overall negligible contribution to lag at a group-level in the studied cohort. To strengthen this, a longitudinal recovery of lag in the lesioned hemisphere shown in this study was not matched by a longitudinal improvement in CVR previously published in the same cohort.²² Thus, the observed hemodynamic latencies are likely to be related to other factors discussed below.

An alternative, but nonmutually exclusive, explanation for the lag may relate to blood flow dynamics. Although measures of hemodynamic lag and blood flow show

no correlation in large cohorts of healthy controls, and regressing out cerebral blood flow has been shown to have a negligible effect on these latencies,² patients may exhibit a different relationship. Indeed correlations between BOLD delay and several perfusion metrics have been shown after hyperacute stroke⁸ and in the subacute phase.⁶ Notably, however, although studies in the hyperacute stroke phase have demonstrated recovery of lag in association with recovery of perfusion, others have not been able to replicate this finding in the subacute phase of stroke.⁶ This suggests that at least in some patients, and/or at different phases of stroke, factors other than blood flow may have a greater contribution to the lag.

In this study, we did not quantitatively measure cerebral blood flow, but since a quarter of the patients had >50% vascular stenosis at the time of the study (Table S1), we were able to test for the effect of vascular stenosis on lag and infer if potentially clinically significant flow restrictions are associated with more hemodynamic lag. The lesioned hemisphere lag was similar in patients with and without 50% stenosis (Figure S5). This accords well with the observation that cerebral blood flow measures

only start to decrease in areas of >2 s lag, (cf. 0.92 s average lag in our study).⁶ Although in the absence of direct perfusion metrics, we are unable to confidently exclude the contribution of blood flow restrictions to the observed lag, these results hint at the assumption that other determinants, which might include neuronal activity, might additionally contribute to the observed lag, in keeping with studies supporting a neural contribution to HRF lag.²

In support of the neural hypothesis, lag measured between homotopic brain regions in patients with stroke was correlated with distance from lesion as well as structural connectivity, suggesting an intrinsic neural architecture.¹¹ Equally the patterns of lag observed in this cohort further support a neural hypothesis for the lag. Both patients and controls showed a similar lag distribution across brain conditions (RS, BH), despite slight regional differences. Although individual patients showed variable and idiosyncratic patterns of lag and lag recovery, the main group difference between patients and controls was increased lag in the perilesional cortices of the left hemisphere, with a lag laterality biased towards the left hemisphere. There was a partial reduction of lag in the lesioned hemisphere over time, in accordance with previous studies.⁶ Without direct measurement of perfusion, it is difficult to disentangle whether group differences seen between patients and controls are due to altered perfusion, or reflect disruption of the distributed left-lateralized brain networks and thus a slower information transfer within these networks. The latter was proposed as the main driving factor for lag observed in a similar cohort of patients following aphasic stroke, where the authors reported extensive behavioral correlations with lag attributed to altered function of brain networks supporting language.⁷ Although we did not find similarly extensive behavioral correlation with lag, a relative lead within the left planum temporale correlated with better fluency performance (Figure S6). A right lateralized hemodynamic signal lead in the occipital lobes in patients (Figure 3A.1), could indicate a redistribution of blood flow after the ischemic insult in other vascular territories.³⁰ Equally, it has been shown that increased occipital hemodynamic lead can be correlated with better behavioral performance in patients poststroke, suggesting that this lead and early engagement may have a compensatory role.⁷

Symmetrical regions of hemodynamic lead were seen in the primary sensorimotor cortices and parietal lobes. Patients showed a similar pattern but a reduced spatial distribution of the hemodynamic lead in the lesioned hemisphere. This accords with previous studies showing reduced hemodynamic lead ipsilaterally.⁷ Further areas of hemodynamic lead were identified in the bilateral precuneus, anterior and posterior cingulate, and lateral occipital cortices, in keeping with previous studies on large cohorts of healthy controls (Mitra and colleagues,² Figure 2C, blue). Our findings of a relative hemodynamic

lag in midline occipito-parietal cortices, middle frontal gyri, and posterior precuneus cortices have also been reported^{2,33} (Mitra et al,² Figure 2C, red).

Animal studies investigating signal propagation have identified motor, sensory and visual cortical areas as sources, where signal arises early and propagates further to posterior and anterior medial sinks.³⁴ This is in keeping with our finding of a relative hemodynamic lead in somatosensory regions and could be driven by higher myelination levels facilitating earlier signal propagation.³⁵ Additional imaging measures of myelination in future studies will be needed to test this hypothesis.

We showed that lag maps derived from the RS and breath-holding data are significantly correlated at group level, irrespective of group, time poststroke, or region. Nevertheless, several regional differences across brain conditions were identified, most notably an increased lead in the breath-holding data (Figure 6C; Table S4) that resemble the multiple demand network³¹ and frontoparietal attentional network involved in task control.³² Since CVR, or indeed blood flow, is unlikely to change over the short temporal window of the fMRI session, the changes in lag latencies during BH compared with RS must largely be neurally driven and may reflect neural engagement of attentional networks required for execution of the breath-holding task. Similar results were found in both time points, with more spatially extensive clusters at the first time point (Table S4) perhaps reflecting the fact that performing the task for the first time is more attentionally demanding. This is in keeping with previous studies that have identified differences in lag latencies with plausible neural focality across brain conditions (eyes open versus eyes closed, before and after cued response, and diurnal states) strengthening the neural hypothesis.²

Patients showed highly variable lesion volumes within the left hemisphere (0.3–168 cm³). Given our previous observation of lower CVR within the lesioned tissue,²² we investigated the effect of lesion volume on the relationship between CVR and lag and did not find it to be a significant confound in this cohort (Figure S7). Equally, lesion volume was not a significant contributor to the number of predominantly white matter located voxels that were excluded from lag calculations (Figure S1).

Our choice of reference signal, against which the lag is measured, is consistent with methods published previously in patients with stroke.^{6,7} We have shown that the pattern of observed lag is unlikely to be affected by the choice of reference signal (Figure S8).

Limitations

A limitation of this study is the inability to directly relate perfusion metrics to HRF lags. However, we did not find an association between the presence of vascular stenosis, (which can potentially cause clinically significant flow restrictions) and larger hemodynamic lags in our

cohort. Future studies combining simultaneous RS EEG fMRI, BH fMRI, and perfusion measures would be ideally placed to disentangle the complex nature of hemodynamic lag and differentiate between neural and vascular contributions to the HRF delay. Relatedly, cerebrovascular reactivity in response to hypercapnia is dependent on the arrival time of the acidic blood to the brain tissue which may be prolonged due to cerebrovascular disease and time taken for local vasodilation of the cerebral microcirculation. Disentangling the 2 without time-based measures of perfusion is difficult.

A further limitation is motion which can be significant in any patient population, particularly during task. We took stringent measures to exclude data frames and subjects with excessive motion.

Although lesioned voxels were not excluded from the group-level analyses investigating between-group lag differences, it is unlikely that their exclusion would have altered the results, as the main areas of significant group differences were confined to brain regions intact in most patients (Figure 3A.3). Accordingly, the maximum area of lesion overlap (lesioned voxels in 8 patients) was in the deep white matter, away from regions of main group differences in lag.

In our study, there was a strong contribution of the transverse venous sinuses to the hemodynamic lag of highest magnitude, as previously described.^{2,36}

Conclusions

Given that fMRI BOLD signal is ubiquitously used to investigate brain-behavior relationships, disentangling the pathophysiology of the temporal delays in the BOLD signal is important for an accurate interpretation of fMRI data. This is most imperative in studies of patients with stroke where neurovascular decoupling is a frequent finding. We show for the first time that previously reported changes in CVR after stroke have a minimal contribution to any observed hemodynamic lag in the BOLD signal. We demonstrate that the temporal lag patterns are spatially correlated across conditions, with any observed differences being plausibly explained by appropriate neural focality. Furthermore, we show that lag patterns share similarities among patients with stroke and controls. Future studies with concurrent EEG, fMRI, and perfusion measures will be better placed to disentangle the relative contribution of perfusion versus neural processes to hemodynamic lag in patients after stroke.

ARTICLE INFORMATION

Received September 12, 2022; final revision received December 2, 2022; accepted December 21, 2022.

Affiliations

Clinical Language and Cognition group, Imperial College London, United Kingdom (A.B., F.G.). Centre for Neuroimaging Science, King's College London, United

Kingdom (R.L.). Cardiff University Brain Research Imaging Centre, School of Physics and Astronomy, Cardiff University, United Kingdom (K.M.).

Acknowledgments

The authors are grateful to all participants who took part in the study.

Sources of Funding

This research was funded in whole, or in part, by the Wellcome Trust (grant numbers: 093957, 200804, 224267). For the purpose of open access, the author has applied a CC BY public copyright license to any Author Accepted Manuscript version arising from this submission.

Disclosures

None.

Supplemental Material

Supplemental Methods
Figures S1–S8
Tables S1–S4
STROBE Checklist

REFERENCES

- Lindquist MA, Meng Loh J, Atlas LY, Wager TD. Modeling the hemodynamic response function in fMRI: efficiency, bias and mis-modeling. *Neuroimage*. 2009;45:S187–S198. doi: 10.1016/j.neuroimage.2008.10.065
- Mitra A, Snyder AZ, Hacker CD, Raichle ME. Lag structure in resting-state fMRI. *J Neurophysiol*. 2014;111:2374–2391. doi: 10.1152/jn.00804.2013
- Amemiya S, Kunimatsu A, Saito N, Ohtomo K. Cerebral hemodynamic impairment: assessment with resting-state functional MR imaging. *Radiology*. 2014;270:548–555. doi: 10.1148/radiol.13130982
- Amemiya S, Kunimatsu A, Saito N, Ohtomo K. Impaired hemodynamic response in the ischemic brain assessed with BOLD fMRI. *Neuroimage*. 2012;61:579–590. doi: 10.1016/j.neuroimage.2012.04.001
- Lv Y, Margulies DS, Cameron Craddock R, Long X, Winter B, Gierhake D, Endres M, Villringer K, Fiebach J, Villringer A. Identifying the perfusion deficit in acute stroke with resting-state functional magnetic resonance imaging. *Ann Neurol*. 2013;73:136–140. doi: 10.1002/ana.23763
- Siegel JS, Snyder AZ, Ramsey L, Shulman GL, Corbetta M. The effects of hemodynamic lag on functional connectivity and behavior after stroke. *J Cereb Blood Flow Metab*. 2016;36:2162–2176. doi: 10.1177/0271678X15614846
- Zhao Y, Lambon Ralph MA, Halai AD. Relating resting-state hemodynamic changes to the variable language profiles in post-stroke aphasia. *Neuroimage Clin*. 2018;20:611–619. doi: 10.1016/j.nicl.2018.08.022
- Khalil AA, Ostwaldt A-C, Nierhaus T, Ganeshan R, Audebert HJ, Villringer K, Villringer A, Fiebach JB. Relationship between changes in the temporal dynamics of the blood-oxygen-level-dependent signal and hypoperfusion in acute ischemic stroke. *Stroke*. 2017;48:925–931. doi: 10.1161/strokeaha.116.015566
- Tong Y, Lindsey KP, Hocke LM, Vitaliano G, Mintzopoulos D, Frederick B. Perfusion information extracted from resting state functional magnetic resonance imaging. *J Cereb Blood Flow Metab*. 2017;37:564–576. doi: 10.1177/0271678X16631755
- Khalil AA, Villringer K, Filleböck V, Hu J-Y, Rocco A, Fiebach JB, Villringer A. Non-invasive monitoring of longitudinal changes in cerebral hemodynamics in acute ischemic stroke using BOLD signal delay. *J Cereb Blood Flow Metab*. 2020;40:23–34. doi: 10.1177/0271678X18803951
- Wang X, Seguin C, Zalesky A, Wong W-W, Chu WC-W, Tong RK-Y. Synchronization lag in post stroke: relation to motor function and structural connectivity. *Netw Neurosci*. 2019;3:1121–1140. doi: 10.1162/netn_a_00105
- Attwell D, Buchan AM, Charpak S, Lauritzen M, Macvicar BA, Newman EA. Glial and neuronal control of brain blood flow. *Nature*. 2010;468:232–243. doi: 10.1038/nature09613
- He F, Sullender CT, Zhu H, Williamson MR, Li X, Zhao Z, Jones TA, Xie C, Dunn AK, Luan L. Multimodal mapping of neural activity and cerebral blood flow reveals long-lasting neurovascular dissociations after small-scale strokes. *Sci Adv*. 2020;6:eaba1933. doi: 10.1126/sciadv.aba1933
- Hall CN, Reynell C, Gesslein B, Hamilton NB, Mishra A, Sutherland BA, O'Farrell FM, Buchan AM, Lauritzen M, Attwell D. Capillary pericytes regulate cerebral blood flow in health and disease. *Nature*. 2014;508:55–60. doi: 10.1038/nature13165

15. Howarth C, Sutherland B, Choi HB, Martin C, Lind BL, Khennouf L, LeDuc JM, Pagan JMP, Ko RWY, Ellis-Davies G, et al. A critical role for astrocytes in hypercapnic vasodilation in brain. *J Neurosci*. 2017;37:2403–2414. doi: 10.1523/JNEUROSCI.0005-16.2016
16. Bright MG, Murphy K. Reliable quantification of BOLD fMRI cerebrovascular reactivity despite poor breath-hold performance. *Neuroimage*. 2013;83:559–568. doi: 10.1016/j.neuroimage.2013.07.007
17. Murphy K, Harris AD, Wise RG. Robustly measuring vascular reactivity differences with breath-hold: normalising stimulus-evoked and resting state BOLD fMRI data. *Neuroimage*. 2011;54:369–379. doi: 10.1016/j.neuroimage.2010.07.059
18. Petersson J, Glenn RW. Gas exchange and ventilation-perfusion relationships in the lung. *Eur Respir J*. 2014;44:1023–1041. doi: 10.1183/09031936.00037014
19. Pinto J, Bright MG, Bulte DP, Figueiredo P. Cerebrovascular reactivity mapping without gas challenges: a methodological guide. *Front Physiol*. 2020;11:608475. doi: 10.3389/fphys.2020.608475
20. Urbach AL, MacIntosh BJ, Goldstein BI. Cerebrovascular reactivity measured by functional magnetic resonance imaging during breath-hold challenge: a systematic review. *Neurosci Biobehav Rev*. 2017;79:27–47. doi: 10.1016/j.neubiorev.2017.05.003
21. Krainik A, Hund-Georgiadis M, Zysset S, von Cramon DY. Regional impairment of cerebrovascular reactivity and BOLD signal in adults after stroke. *Stroke*. 2005;36:1146–1152. doi: 10.1161/01.STR.0000166178.40973.a7
22. Geranmayeh F, Wise RJS, Leech R, Murphy K. Measuring vascular reactivity with breath-holds after stroke: a method to aid interpretation of group-level BOLD signal changes in longitudinal fMRI studies. *Hum Brain Mapp*. 2015;36:1755–1771. doi: 10.1002/hbm.22735
23. Geranmayeh F, Leech R, Wise RJS. Network dysfunction predicts speech production after left hemisphere stroke. *Neurology*. 2016;86:1296–1305. doi: 10.1212/WNL.0000000000002537
24. Geranmayeh F, Chau TW, Wise RJS, Leech R, Hampshire A. Domain-general subregions of the medial prefrontal cortex contribute to recovery of language after stroke. *Brain*. 2017;140:1947–1958. doi: 10.1093/brain/awx134
25. Stefaniak JD, Geranmayeh F, Lambon Ralph MA. The multidimensional nature of aphasia recovery post-stroke. *Brain*. 2022;145:1354–1367. doi: 10.1093/brain/awab377
26. Jenkinson M, Bannister P, Brady M, Smith S. Improved optimization for the robust and accurate linear registration and motion correction of brain images. *Neuroimage*. 2002;17:825–841. doi: 10.1016/s1053-8119(02)91132-8
27. Power JD, Barnes KA, Snyder AZ, Schlaggar BL, Petersen SE. Spurious but systematic correlations in functional connectivity MRI networks arise from subject motion. *Neuroimage*. 2012;59:2142–2154. doi: 10.1016/j.neuroimage.2011.10.018
28. Bonakdarpour B, Parrish TB, Thompson CK. Hemodynamic response function in patients with stroke-induced aphasia: implications for fMRI data analysis. *Neuroimage*. 2007;36:322–331. doi: 10.1016/j.neuroimage.2007.02.035
29. de Haan B, Rorden C, Karnath H-O. Abnormal perilesional BOLD signal is not correlated with stroke patients' behavior. *Front Hum Neurosci*. 2013;7:669. doi: 10.3389/fnhum.2013.00669
30. Thompson CK, Walenski M, Chen Y, Caplan D, Kiran S, Rapp B, Grunewald K, Nunez M, Zinbarg R, Parrish TB. Intrahemispheric perfusion in chronic stroke-induced aphasia. *Neural Plast*. 2017;2017:2361691. doi: 10.1155/2017/2361691
31. Duncan J. The multiple-demand (MD) system of the primate brain: mental programs for intelligent behaviour. *Trends Cogn Sci*. 2010;14:172–179. doi: 10.1016/j.tics.2010.01.004
32. Dosenbach NUF, Fair DA, Miezin FM, Cohen AL, Wenger KK, Dosenbach RAT, Fox MD, Snyder AZ, Vincent JL, Raichle ME, et al. Distinct brain networks for adaptive and stable task control in humans. *Proc Natl Acad Sci USA*. 2007;104:11073–11078. doi: 10.1073/pnas.0704320104
33. Mitra A, Snyder AZ, Blazey T, Raichle ME. Lag threads organize the brain's intrinsic activity. *Proc Natl Acad Sci USA*. 2015;112:E2235–E2244. doi: 10.1073/pnas.1503960112
34. Mohajerani MH, Chan AW, Mohsenvand M, LeDuc J, Liu R, McVea DA, Boyd JD, Wang YT, Reimers M, Murphy TH. Spontaneous cortical activity alternates between motifs defined by regional axonal projections. *Nat Neurosci*. 2013;16:1426–1435. doi: 10.1038/nn.3499
35. Glasser MF, Coalson TS, Robinson EC, Hacker CD, Harwell J, Yacoub E, Uğurbil K, Andersson J, Beckmann CF, Jenkinson M, et al. A multi-modal parcellation of human cerebral cortex. *Nature*. 2016;536:171–178. doi: 10.1038/nature18933
36. Hall DA, Gonçalves MS, Smith S, Jezzard P, Haggard MP, Kornak J. A method for determining venous contribution to BOLD contrast sensory activation. *Magn Reson Imaging*. 2002;20:695–706. doi: 10.1016/s0730-725x(02)00607-0